Front. Phys. 10, 104203 (2015)
DOI 10.1007/s11467-014-0439-8

RESEARCH ARTICLE

Fano resonances in complex plasmonic super-nanoclusters: The effect of environmental modifications on the LSPR sensitivity

Arash Ahmadivand[1,†], **Saeed Golmohammadi**[2]

[1] *Young Researchers and Elite Club, Ahar Branch, Islamic Azad University, Ahar, Iran*
[2] *School of Engineering-Emerging Technologies, University of Tabriz, Tabriz 5166614761, Iran*
Corresponding Author. E-mail: [†] *a_ahmadivand@iau-ahar.ac.ir*
Received May 1, 2014; accepted June 30, 2014

In this study, gold nanodisk clusters in heptamer orientations as clusters were used to design a super-heptamer consisting of one central and six peripheral heptamers. We examined the position and movement of the plasmon and Fano resonances by sketching the spectral response of the superstructure for various nanodisk dimensions. The quality of the interference between the superradiant and subradiant plasmon resonance modes of the nanodisk clusters was found to depend strongly on the structural configuration and the refractive index of the environmental medium. We replaced the central heptamer with a nanodisk and probed the position of the Fano resonance by geometrically altering the nanodisk structure. Finally, the effect of the dielectric environment on the plasmon response of both of the studied structures was examined numerically and theoretically. The localized surface plasmon resonance sensitivity of the finite plasmonic structures to the presence of liquid substances was investigated and shown by plotting the linear figure of merit. The finite-difference time-domain method was used as a numerical tool to investigate the plasmon response of the structure.

Keywords gold nanodisk, spectral response, Fano resonance, localized surface plasmon resonance (LSPR), figure of merit (FoM).

PACS numbers 42.79.-e, 73.20.Mf

Frontiers of Physics

1 Introduction

Localized surface plasmon resonances (LSPRs) in nanoscale noble metal structures have been broadly investigated in most recent publications on the topic [1–5]. The plasmonic resonances can be spectrally tuned by controlling the structural and compositional properties of the metallic configurations and embedded medium [6–10]. Recent works have extensively studied mostly simple and composite metallic nanoclusters, such as dimers [11–14], trimers [15–17], quadrumers [18], heptamers [19–22], tetramers [23], and oligomers [24], where the nanoclusters are commonly presented in two- and three-dimensional regimes to exploit the manipulation of novel blueprints. Each of the nanocluster types above exhibits particular unique collective plasmon and Fano resonance modes that arise from constructive interaction and coupling between the plasmon modes of adjacent metallic nanoparticles inside the cluster aggregate. Collective and coherent plasmon resonance modes can be excited at different optical powers (in eV) that depend strongly on the corresponding plasmon resonance fluctuations in individual nanoparticles. These close and intense interactions of plasmon modes can be analyzed using plasmon hybridization theory [25–28]. Using this theory, we can characterize the multicomponent plasmon modes in complex nanostructures and nanoclusters. For instance, Prodan *et al.* [25] and Fan *et al.* [20] proved that a plasmonic heptamer in a symmetric molecular (benzene) regime can be tailored to support strong magnetic plasmon resonance and Fano resonance originating from the constructive interference of hybridized bright (superradiant) and dark (subradiant) plasmon resonance modes. The spectral response of these particle clusters depends strongly on the coherence of the interfering resonance modes; consequently, minor derangements differences in the physical and chemical properties of clusters and the surrounding medium, such as the shape of the utilized nanoparticles, symmetry cancellation, and sub-

stance modifications, directly and dramatically affect the plasmon response of the proposed configuration. Spheres [30], disks [31], shells [32], pyramids [33], core-shells [34], and ellipsoids [35] have been employed extensively as subwavelength nanoparticles in designing various orientations of sef-assembled clusters and associated particle networks to support plasmon and Fano resonances efficiently. On the other hand, remarkable efforts have been made recently to develop the concept of Fano resonance, and it is shown that Fano resonance can be employed to design practical and applicable plasmonic Fano switches [36], nanoantennas [37], LSPR sensors [38], and (de)multiplexers [39].

In this work, we examine the plasmonic properties and spectral response of a super-heptamer composed of one central and six identical peripheral heptamers that are separated by an identical gap of D_{7h}. The distances of the nanoparticles in a cluster from each other and from those in each of the adjacent heptamers are equal. The design of the proposed heptamers is based on gold nanodisks with experimentally calculated Johnson–Christy constants [40, 41] that are situated 12 nm ($D_{7h} = 12$ nm) from nearby particles. This work also describes the effect of the medium material and the sizes of the nanoparticles on the scattering spectra and plasmon response, especially for the LSPR sensing approaches. It is shown that the examined heptamer assembly is highly sensitive to chemical and structural alterations that directly influence the Fano resonance wavelength position. Therefore, we measured the effect of controlled symmetry cancellation in the superstructure by replacing the central heptamer with a large nanodisk. Additionally, the effect of modifications in the medium material on the scattering intensity was evaluated numerically for both of the proposed nanostructures. The Fano resonance shift and minimum depth were compared with those of other analogous nanostructures, and the corresponding figure of merit (FoM) for the LSPR response was calculated and demonstrated using a diagram. The proposed superstructures open new paths to the design of enhanced high-sensitivity devices such as biosensors, surface-enhanced Raman spectroscopy (SERS) devices, and efficient Fano switches. The finite-difference time-domain (FDTD) method [42, 43] was considered as a numerical model to extract and evaluate the optical properties of the examined structures.

2 Results and discussion

Figure 1(a) shows a three-dimensional schematic diagram of the proposed configuration based on gold nanodisk heptamers, the orientation of which resembles a super-heptamer. Note that two adjacent nanoparticles supply strong resonance coupling between nearby clusters within the structure. It is well known that because of the inherent symmetry of heptamer structures, the frequency of coupled plasmon modes for two adjacent particles in a symmetric regime can be written as [34]

$$\omega_l^2 = \frac{\omega_B^2}{2}\left(1 - \frac{1}{2l+1}\sqrt{1+4l(l+1)r^{2l+1}}\right), \qquad (1)$$

where l is the energy level corresponding to a bonding mode, and r is the radius of the gold nanodisk. Using an electric dipole source located to the left of the super-heptamer, we excited surface plasmon resonances (SPRs) through the arrays of nanoparticles. In terms of the Fano resonance, two fundamental modes are involved: interference of the superradiant mode (bonding bright mode), which corresponds to the in-phase oscillations of the dipolar plasmons of all the nanoparticles, and on the other hand, subradiant (antibonding dark mode) modes that are related to the plasmon dipolar moment of the central components (here, the central heptamer), which oscillates in the direction opposite to the nearby particles' moments [29]. Here, we used a heptamer of nanodisks for each of the central and peripheral particles. It is well understood that in the nonretarded limit, the subradiant mode cannot be coupled to the superradiant mode efficiently, and on the other side, in the retarded limit, an interaction between the dark and bright modes occurs that contains a Fano resonance in the bright continuum at the energy level of the bright mode [29, 44]. Employing the FDTD method as a numerical tool, we demonstrated the effect of changes in the nanodisk size on the scattering cross-section diagram for the proposed super-heptamer under illumination by an incident dipole source. Gold particles are deposited on a glass substrate (default substrate) with a permittivity of $\varepsilon \sim 2.1$, and the gap sizes between all of the nanoparticles in the seven heptamers is set to 12 nm; this distance will remain fixed during geometrical alterations in all of the other regimes discussed later. To show the effect of geometrical modifications on the Fano resonance behavior, we increased the radii of all of the nanodisks (central and peripheral) from 55 nm to 90 nm simultaneously, while the distance between them remained unchanged. Figure 1(b) demonstrates the scattering cross-section transition from the quasi-static limit to the completely retarded limit, which affects the Fano resonance minimum dramatically. This figure shows the spectral response of the smallest super-heptamer (nanodisks with radii of 55 nm); we detected a plasmon resonance extreme representing superradiant bonding at $\lambda \sim 1045$ nm and a Fano minimum mode

at $\lambda \sim 1190$ nm. When the radii of the nanodisks was increased to 75 nm, a Fano minimum appeared at $\lambda \sim 1280$ nm, which shows a strong red-shift of the subradiant modes compared to the superradiant ones because of the existence of quadrupole and higher-order poles (multipoles) in the subradiant modes. As we expected, increasing the size of the heptamer arrays directly enhances the intensity of the interacting plasmon resonance modes, and this regime directly causes dramatic red-shifts in the position of the subradiant dark mode compared to that of the superradiant bright mode. For the heptamers composed of nanodisks with radii of 90 nm, the Fano resonance minimum appears at $\lambda \sim 1325$ nm; it is narrower than those in the previous regimes and is completely red-shifted to the edge of the NIR region. However, the Fano depth is reduced, and this condition

Table 1 FDTD parameter descriptions and settings to investigate the optical response of the examined superstructures.

FDTD parameter description	Quantities/Situation
Cell numbers	200 000
Spatial cell size ($dx = dy = dz$)	0.01 nm
Number of time step (dt)	17 000
Number of snapshots	28 250
Simulation time	5 500 (fs)
Background index	1
Boundary conditions	PML (Perfectly matched layers)
Number of PML layers	16
Dipole source amplitude	2.190 59e-31
Pulse length	2.653 35(fs)
Offset	7.523 11(fs)

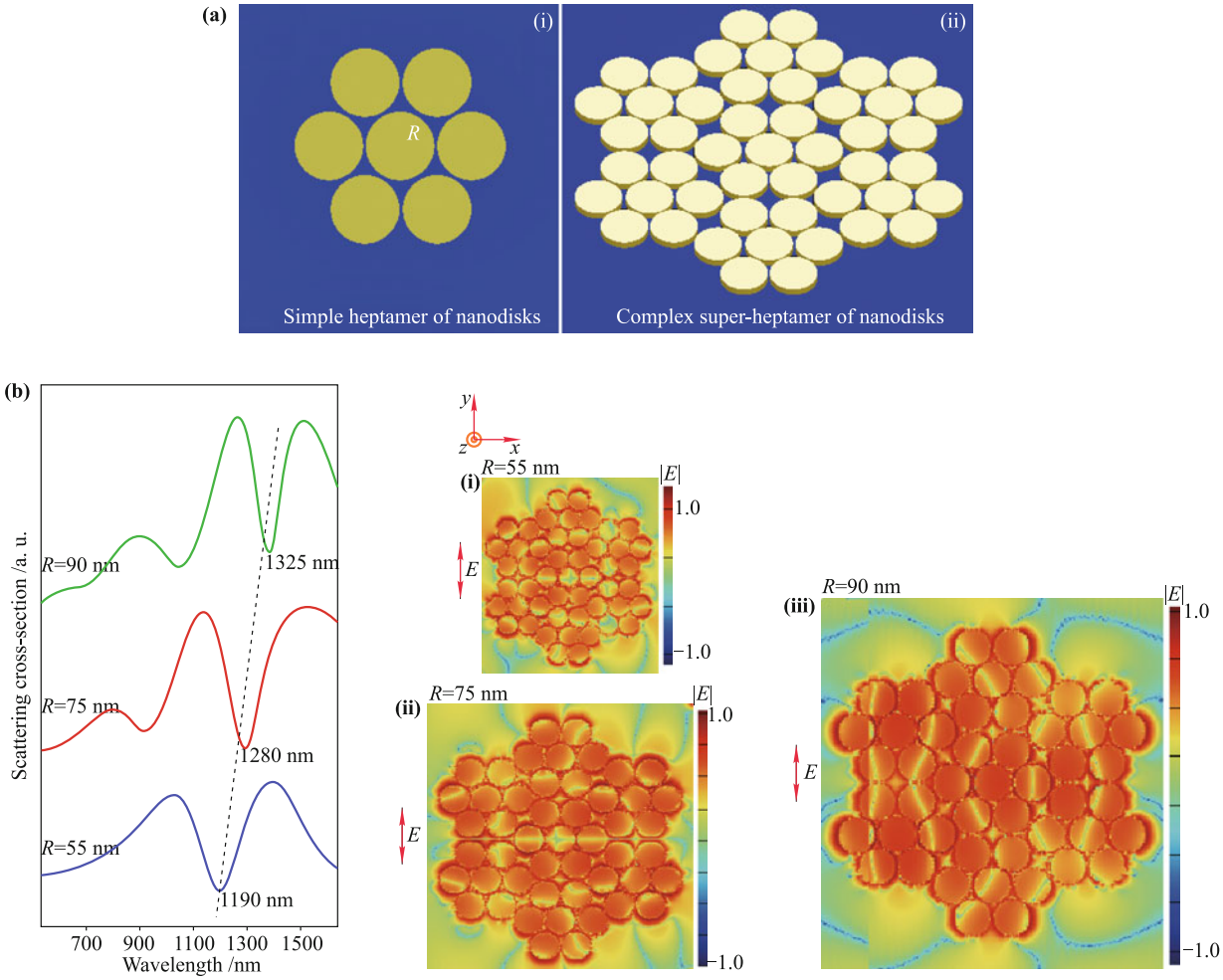

Fig. 1 **(a)** (i) The schematic art of the simple heptamer based on gold nanoparticles is illustrated which are deposited on a glass substrate. (ii) Complex super-structure based on a central heptamer of nanodisks and six spherical heptamers is demonstrated artificially. **(b)** Illuminating the super-structure of heptamers by an electric dipole source, we sketched the scattering spectra for the configuration and the plasmon resonance and Fano minima are appeared for nanodisks with radii of R=55 nm (i). Increasing the size of nanodisks to 75 nm, the Fano minima red-shifted and became narrower and deeper (ii). Setting the nanodisks radiuses to 90 nm, we observed the Fano minima at $\lambda \sim 1325$ nm (red-shifted), but its depth is reduced (iii). Inset snapshots illustrate the quality of plasmon resonance coupling between proximal heptamers.

is not favorable. This behavior is attributed to the high ratio of damping or internal absorption of the incident electromagnetic field by Au nanodisks with large radii. Accordingly, finding suitable nanoparticle dimensions on the basis of their spectral response can help us to design an efficient subwavelength structure. Thus, in the remainder of the paper, we will consider radii smaller than 90 nm (e.g., 85 nm) to prevent an undesirable amount of light absorption and to provide deep, narrow Fano resonance minima that exhibit the desired red-shift. The inset snapshots in Fig. 1(b) (i–iii) demonstrate two-dimensional $(x - y)$ simulation images of robust SPR excitation and coupling between clusters and particles. A comparison with a simple nanoparticle heptamer cluster reveals that in the proposed complex heptamer-based structure, the quality of the Fano minimum has switched to strong Fano resonance from the Fano-like regime. This capability is attributed to constructive and weak interference of the sub- and superradiant dipolar plasmon resonance mode extremes for the super-heptamer.

Next, we studied the results of modifications in the shape of the super-heptamer components on the spectral response of this configuration. Figure 2(a) illustrates the modified version of the structure in which the central heptamer was replaced by a large nanodisk (360 nm in radius), and the dimensions of the peripheral heptamers, which are composed of nanodisks with radii of 85 nm, remain unchanged. This geometrical alteration will help us to provide the required asymmetry for Fano resonance formation along the scattering spectra simply. Figure 2(b) shows a two-dimensional $(x - y)$ snapshot of SPR excitation and coupling between nearby particles and heptamers. Because of the outstanding and inherent symmetry of the structure, the position of the employed particles, the angle of the incident light, and the configuration rotation do not significantly affect the scattering efficiency, and these results are depicted in Fig. 2(c) for incident light with different angles and polarizations (ϕ) of 0°, 45°, or 90°. Owing to this initial symmetry in the structural components of the large heptamer, therefore, we investigated the optical response of the structure to different polarizations as a major parameter merely to draw the scattering efficiency profile numerically. In this regime, the position of the Fano resonance is blue-shifted ($\lambda \sim 1370$ nm); the polarization direction does not significantly affect the Fano resonance shifting and quality, and causes minor variations in the amplitude of the scattering spectra. The detected minima along the diagram indicate the subradiant dark mode. Considering the position of the superradiant bright mode ($\lambda \sim 1110$ nm), we would be able to calculate and draw the charge density distribution within and between the Au nanodisks. Accordingly, because of the constructive interference of radiated plasmon resonance modes that originate in the symmetry of the proposed superstructure, the charge density distribution directions in all of the nanoparticles are the same; this situation resembles the in-phase mode. The charge density distribution plot for the super-heptamer at the subradiant dark mode (at $\lambda \sim 1415$ nm) shows that this mode supports charge oscillations within the structure in different directions (out-of-phase mode) caused by interference of radiated dark and bright plasmon resonance modes [Fig. 2(a)]. To provide a comprehensive study, we modified the geometries of the structure to supply the asymmetry required to enhance the quality of the Fano dip. This situation helps us to examine the optical response of the structure during the transition from the symmetric to the antisymmetric regime.

To this end, we reduced the size of the central nanodisk to break the symmetry of the superstructure while keeping the radii of the disks in the peripheral heptamers fixed at 85 nm. Technically, reducing the size of the central nanodisk disrupts the structure by decreasing the size of the gap between nearby particle units; this affects the performance of the structure dramatically by changing the quality of the Fano resonance and the resonance hybridization strength. Figure 3(a) shows the results of a numerical calculation using the FDTD method that demonstrates the effect of decreasing the central disk radius on the scattering efficiency and the position of the Fano resonance minimum. Obviously, this reduction directly blue-shifts the Fano dip. In this regime, we observed highly pronounced Fano minima due to the presence of peripheral heptamers, which cancel the dipole moment of the nanoparticle clusters (bright mode), while the central nanodisk provides the subradiant dark mode. In the proposed structure, the antibonding mode remains subradiant, and a robust Fano resonance dip is induced by all of the structural modifications; this dip cannot be observed in analogous structures such as octamers in both homo and hetero regimes. To prove this claim, we reduced the size of the central nanodisk from 340 nm to 200 nm. Changing the structure from the homo-regime to the hetero-regime does not affect the presence of the Faro minimum, but blue-shifts its position and broadens it. In addition, the dipole moment is completely coupled to the incident light because it remains equal to the moments of the surrounding heptamers. To provide a comprehensive investigation, we altered the size of the nanodisks in the peripheral heptamers while keeping the size of the central nanodisk unchanged at 360 nm. Figure 3(b) numerically demonstrates the effect of these variations on the existence and position of the Fano resonance.

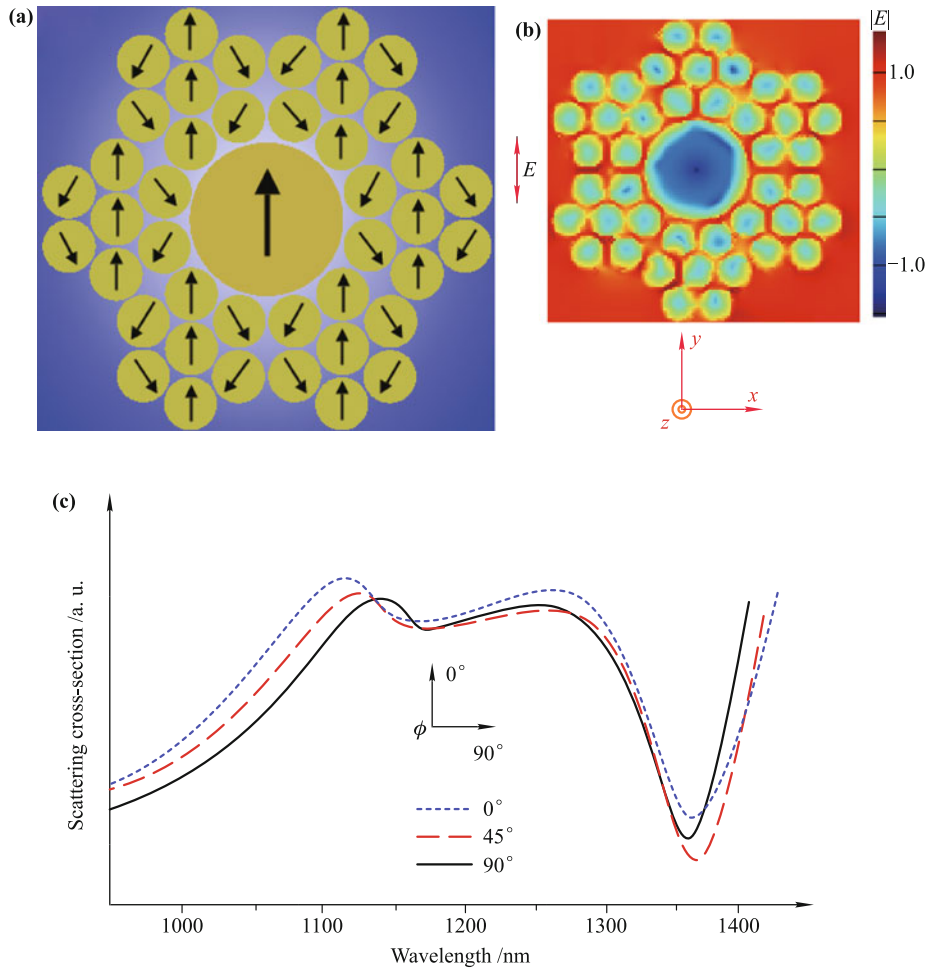

Fig. 2 **(a)** Schematic art of the super-heptamer based on central nanodisk and six peripheral clusters, this picture includes the direction of charge oscillations. **(b)** A two-dimensional snapshot (x–y view) of plasmon resonance excitation and coupling between proximal clusters of super-structure. **(c)** Scattering cross-sectional diagram is illustrated for examined super-structure under transverse electric mode excitation with three different orientation angles. The peak resonance of the superradiant bright mode is observed at $\lambda\sim1110$ nm and the charge oscillations direction in all of the nanodisks is same. The Fano resonance dip is observed at $\lambda\sim1370$ nm.

Subtle increments in the size of the surrounding nanodisks directly red-shift the Fano resonance; further, the curve becomes narrower, and a superradiant bright mode appears with these increments. In this case, for nanodisks with radii of $R = 105$ nm, the Fano dip appeared at $\lambda \sim 1345$ nm. This narrow Fano minimum helps us to provide highly precise and sensitive nanostructures, which allow for a more rigorous evaluation of extremely minor movements of resonances that are induced by modifications in the local dielectric properties that appear in the NIR spectra.

In terms of the practical exploitation of Fano resonance, plasmonic Fano switches, demultiplexers, and LSPR sensors [45-47] based on this aspect of optical physics have been reported. Most previous works have examined the effect of environmental modifications on the spectral response of the simple heptamers, oligomers, octamers, and so on that were discussed in the previous section. It is well understood that to evaluate the efficiency of the LSPR sensing of a finite plasmonic nanostructure, the FoM must be determined and drawn [48, 49]. Sherry *et al.* [49] verified that the FoM for a given finite plasmonic subwavelength structure can be quantified by calculating the ratio of the plasmon energy deviation (ΔE, in eV) to the change in the medium's refractive index (n) divided by the cross-sectional peak width. In addition, Hao *et al.* [50] proved that the plasmon resonance energy for the antisymmetric Fano resonances can be determined by finding the midpoint across the energy of the first maximum and minimum through the spectral curve, which provides the energy width.

Next, we numerically plotted the scattering spectra for both of the studied superstructures immersed in the following media: CH_3COCH_3 (acetone), $n = 1.351$;

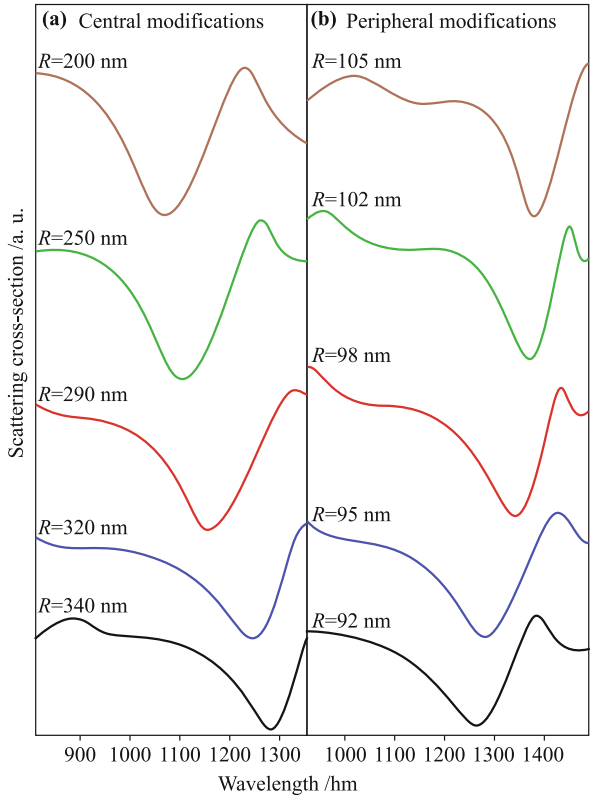

Fig. 3 The scattering spectra is demonstrated for the superstructure based on central big nanodisk. **(a)** The effect geometrical alterations in the central component on the spectral response of the structure is sketched while the radius of the big nanodisk is reducing. This reduction of the disk radii blue-shifted the Fano minima to shorter spectra and become broader which refers to the symmetry breaking regime. **(b)** The effect of geometrical alterations in the peripheral nanodisk clusters on the scattering efficiency is depicted. Increasing the size of nanodisk radiuses red-shifts the Fano minima dramatically and the Fano minima become narrower and deeper.

$C_4H_{10}O$ (butanol), $n = 1.399$; and BK7 matching liquid (similar to Cargille immersion oil type B, which is measured in the Cargille laboratory), $n = 1.516$. In all of the simulations of the supercluster, the proposed structures are deposited on a quartz substrate and thoroughly immersed in one of the above liquids. Figure 4(a) shows the scattering cross-section diagram for the superstructure with a central heptamer composed of gold nanodisks that is surrounded by six peripheral heptamers. All the employed gold nanodisks have radii of 85 nm; obviously, increasing the refractive index of the medium directly red-shifts the Fano minimum robustly and provides a deep Fano minimum at $\lambda \sim 1385$ nm for the medium with a refractive index of $n = 1.516$. Figure 4(b) shows the same scattering spectra diagram for a super-heptamer composed of a central nanodisk 360 nm in radius with six peripheral heptamers with the radii of 80nm. The radii of the nanodisks are chosen to provide a desirable Fano resonance minimum (this situation leads to the formation of an isotropic Fano resonance). As we expected, because of the unique shape of the proposed configuration, which was discussed above, the Fano minimum was red-shifted with increasing refractive index of the surrounding medium. This shift in the Fano resonance is remarkably greater than that in the previous regime and provides a deeper and narrower Fano dip at $\lambda \sim 1560$ nm. To determine the sensitivity of LSPR sensing for both of these superstructures, we divided the slope of the linear regression by the Fano line width of 0.067 eV (0.061 eV), which yielded FoM values of 13.6 (14.2) [Figs. 4(c) and 4(d), respectively] for the entirely heptamer-based superstructure (central disk superstructure). Compared to the LSPR sensitivity of analogous nanostructures, the LSPR sensitivity of the examined configurations of the proposed super-heptamers is noticeable and highly interesting. These finite super-heptamers yield precise LSPR sensing capability by centering on the Fano resonance position and minimum depth. The proposed clusters of heptamers can be fabricated lithographically with smaller gaps between the ensembles of nanodisks to provide more accuracy in sensing applications. The sensitivity of the proposed nanostructure is clearly superior to that of structures reported in previous works. For instance, Lassiter *et al.* [12] has shown that an octamer cluster composed of Au nanodisks in symmetric and asymmetric orientations can provide remarkable Fano dips along the scattering spectral profile with a maximum FoM of 5.7. Moreover, Liu *et al.* [51] has verified that coupled dipole–quadrupole nanoantennas yield an FoM of 3.8. Therefore, the proposed nanostructure offers strong sensitivity for various sensing and SERS applications.

3 Conclusions

In this work, we examined different novel shapes of plasmonic nanoclusters that can be used to design subwavelength configurations for various optical applications from sensing to switching. Gold nanodisk heptamer clusters are the key components of the examined configurations. When a heptamer-based structure consisting of seven heptamers was illuminated by an electric dipole source, pronounced Fano resonances were induced, as shown by the scattering cross-section profile of the structure, and we showed that the position and width of the Fano minimum are highly sensitive to differences in the structure and local medium. Then, we replaced the central heptamer of the superstructure with a large gold nanodisk and studied the effect of this substitution on

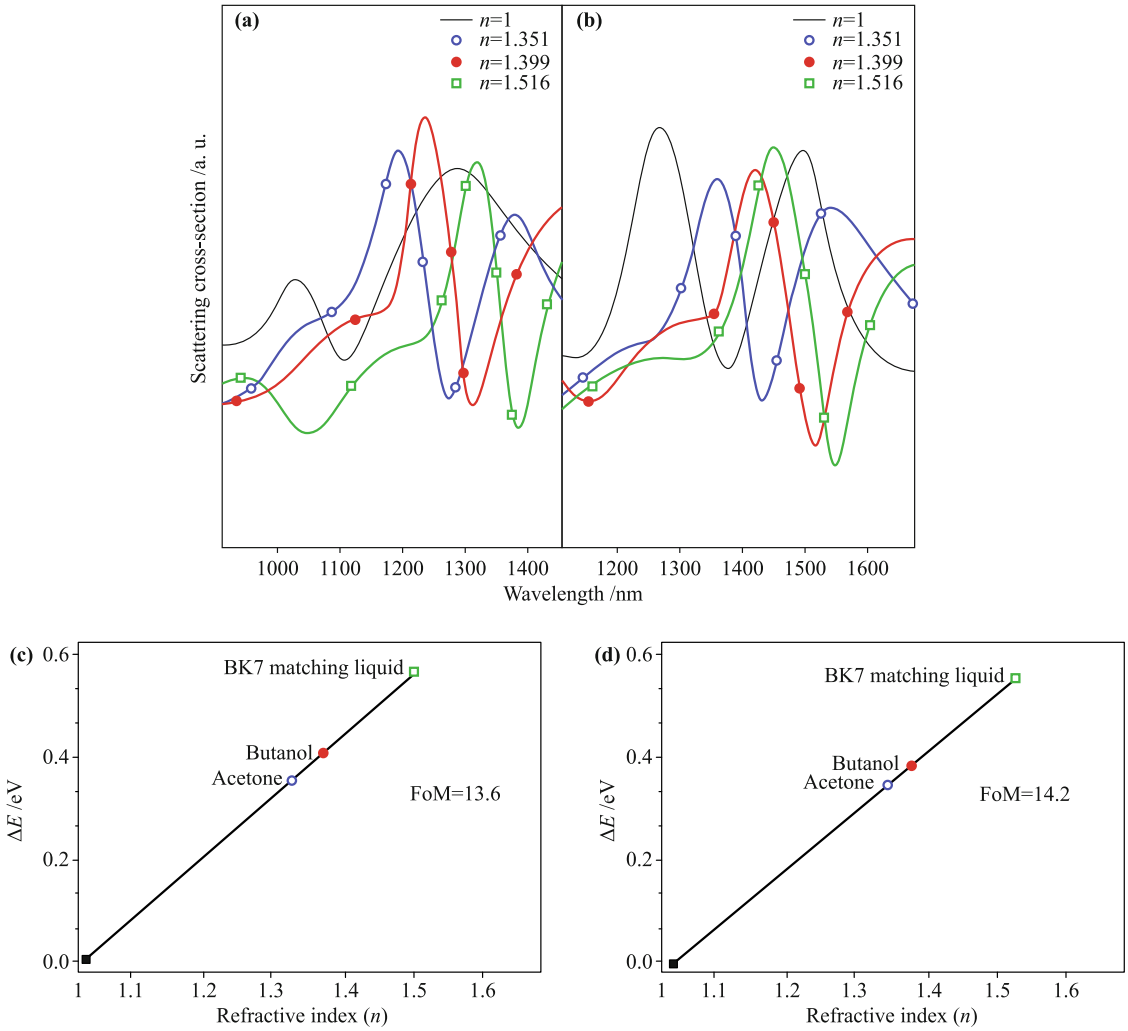

Fig. 4 LSPR sensitivity in proposed super-heptamers is presented. **(a)** LSPR sensing for a super-structure based on seven nanodisks heptamers with the radii size of 85 nm is investigated numerically based on FDTD simulation method. The Fano minima is red-shifted and get narrower by increasing the refractive index of the environmental substance (for three different substances). **(b)** LSPR sensing for a super-structure based on six peripheral nanodisks heptamers and central nanodisk is examined. The Fano minima is red-shifted to larger wavelength by increasing the refractive index of environmental substance. The quality of sensing is improved in this regime based on the Fano minima depth and shifting distance. **(c, d)** Linear plots of the LSPR shifts of the Fano resonance over the refractive index of environmental substances to measure the FoMs for completely heptamer-based-structure and central disk replaced super-structure.

the coupling strength of the subradiant dark and superradiant bright modes and also the position and quality of the Fano resonance. In this regime, we altered the geometrical sizes of the central and peripheral nanodisks to enhance the Fano resonance depth and performance. In addition, we verified that reducing the size of the central nanodisk blue-shifts the Fano minimum; this situation resembles a symmetry-breaking regime. In contrast, increasing the size of the peripheral nanodisks red-shifts the Fano minimum to the edge of the NIR region because of the tendency to offset the asymmetry. Ultimately, using various dielectric substances with different refractive indices as environmental variables, we probed the LSPR sensitivity for both of the examined superstructures on the basis of the corresponding calculated FoM. We quantified the FoM of the entirely heptamer-based superstructure as 13.6, and that of the superstructure with a central nanodisk instead of a heptamer as 14.2. These results proved that the proposed structures have strong potential for use in designing ultrasensitive LSPR sensing devices and nanostructures with high sensitivity and accuracy.

References

1. H. Raether, Surface Plasmons on Smooth and Rough Surfaces and on Gratings; Berlin: Springer-Verlag, 1988

2. U. Kreibig and M. Vollmer, Optical Properties of Metal Clusters, Berlin: Springer-Verlag, 1995
3. B. E. A. Saleh and M. C. Tiech, Fundamentals of Photonics, New York: Wiley, 1991
4. S. A. Maier, Plasmonics: Fundamentals and Applications, New York: Springer, 2007
5. W. L. Barnes, A. Dereux, and T. W. Ebbesen, Surface plasmon subwavelength optics, *Nature* 424(6950), 824 (2003)
6. D. K. Gramotnev and S. I. Bozhevolnyi, Plasmonics beyond the diffraction limit, *Nat. Photonics* 4(2), 83 (2010)
7. J. J. Mock, D. R. Smith, and S. Schultz, Local refractive index dependence of plasmon resonance spectra from individual nanoparticles, *Nano Lett.* 3(4), 485 (2003)
8. S. Linic, P. Christopher, and D. B. Ingram, Plasmonic-metal nanostructures for efficient conversion of solar to chemical energy, *Nat. Mater.* 10(12), 911 (2011)
9. J. B. Pendry, A. Aubry, D. R. Smith, and S. A. Maier, Transformation optics and subwavelength control of light, *Science* 337(6094), 549 (2012)
10. J. Zhu, J. J. Li, L. Yuan, and J. W. Zhao, Optimization of three-layered Au–Ag bimetallic nanoshells for triple-bands surface plasmon resonance, *J. Phys. Chem. C* 116(21), 11734 (2012)
11. C. Y. Tsai, J. W. Lin, C. Y. Wu, P. T. Lin, T. W. Lu, and P. T. Lee, Plasmonic coupling in gold nanoring dimers: observation of coupled bonding mode, *Nano Lett.* 12(3), 1648 (2012)
12. B. Lassiter, J. Aizpurua, L. I. Hernandez, D. W. Brandl, I. Romero, S. Lal, J. H. Hafner, P. Nordlander, and N. J. Halas, Close encounters between two nanoshells, *Nano Lett.* 8(4), 1212 (2008)
13. L. Cheng, J. Song, J. Yin, and H. Duan, Self-assembled plasmonic dimers of amphiphilic gold nanocrystals, *J. Phys. Chem. Lett.* 2(17), 2258 (2011)
14. S. S. Aćmović M. P. Kreuzer, M. U. González, and R. Quidant, Plasmon near-field coupling in metal dimers as a step toward single-molecule sensing, *ACS Nano* 3(5), 1231 (2009)
15. D. W. Brandl, N. A. Mirin, and P. Nordlander, Plasmon modes of nanosphere trimers and quadrumers, *J. Phys. Chem. B* 110(25), 12302 (2006)
16. P. K. Jain and M. A. El-Sayed, Surface plasmon coupling and its universal size scaling in metal nanostructures of complex geometry: Elongated particle pairs and nanosphere trimers, *J. Phys. Chem. C* 112(13), 4954 (2008)
17. L. Chuntonov and G. Haran, Trimeric plasmonic molecules: The role of symmetry, *Nano Lett.* 11(6), 2440 (2011)
18. J. A. Fan, K. Bao, C. Wu, J. Bao, R. Bardhan, N. J. Halas, V. N. Manoharan, G. Schvets, P. Nordlander, and F. Capasso, Fano-like interference in self-assembled plasmonic quadrumer clusters, *Nano Lett.* 10(11), 4680 (2010)
19. J. A. Fan, K. Bao, L. Sun, J. Bao, V. N. Manoharan, P. Nordlander, and F. Capasso, Plasmonic mode engineering with templated self-assembled nanoclusters, *Nano Lett.* 12(10), 5318 (2012)
20. J. A. Fan, C. H. Wu, K. Bao, J. M. Bao, R. Bardhan, N. J. Halas, V. N. Manoharan, P. Nordlander, G. Shvets, and F. Capasso, Self-assembled plasmonic nanoparticle clusters, *Science* 328(5982), 1135 (2010)
21. N. Liu, S. Mukherjee, K. Bao, Y. Li, L. V. Brown, P. Nordlander, and N. J. Halas, Manipulating magnetic plasmon propagation in metallic nanocluster networks, *ACS Nano* 6(6): 5482 (2012)
22. B. Luk'yanchuk, N. I. Zheludev, S. A. Maier, N. J. Halas, P. Nordlander, H. Giessen, and C. T. Chong, The Fano resonance in plasmonic nanostructures and metamaterials, *Nat. Mater.* 9(9), 707 (2010)
23. Z. Fan, H. Zhang, and A. O. Govorov, Optical properties of chiral plasmonic tetramers: Circular dichroism and multipole effects, *J. Phys. Chem. C* 117(28), 14770 (2013)
24. B. Hopkins, A. N. Poddubny, A. E. Miroshnichenko, and Y. S. Kivshar, Revisiting the physics of Fano resonances for nanoparticle oligomers, *Phys. Rev. A* 88(5), 053819 (2013)
25. E. Prodan, C. Radloff, N. J. Halas, and P. Nordlander, A hybridization model for the plasmon response of complex nanostructures, *Science* 302(5644), 419 (2003)
26. P. Nordlander, C. Oubre, E. Prodan, K. Li, and M. I. Stockman, Plasmon hybridization in nanoparticle dimers, *Nano Lett.* 4(5), 899 (2004)
27. H. Liu, D. A. Genov, D. M. Wu, Y. M. Liu, Z. W. Liu, C. Sun, S. N. Zhu, and X. Zhang, Magnetic plasmon hybridization and optical activity at optical frequencies in metallic nanostructures, *Phys. Rev. B* 76(7), 073101 (2007)
28. M. Liu, T. W. Lee, S. K. Gray, P. Guyot-Sionnest, and M. Pelton, Excitation of dark plasmons in metal nanoparticles by a localized emitter, *Phys. Rev. Lett.* 102(10), 107401 (2009)
29. Z. Nie, A. Petukhova, and E. Kumacheva, Properties and emerging applications of self-assembled structures made from inorganic nanoparticles, *Nat. Nanotechnol.* 5, 15 (2010)
30. E. Prodan and P. Nordlander, Plasmon hybridization in spherical nanoparticles, *J. Chem. Phys.* 120(11), 5444 (2004)
31. Y. Sonnefraud, N. Verellen, H. Sobhani, G. A. E. Vandenbosch, V. V. Moshchalkov, P. Van Dorpe, P. Nordlander, and S. A. Maier, Experimental realization of subradiant, superradiant, and fano resonances in ring/disk plasmonic nanocavities, *ACS Nano* 4(3), 1664 , 2010)
32. J. Ye, P. Van Dorpe, L. Lagae, G. Maes, and G. Borghs, Observation of plasmonic dipolar anti-bonding mode in silver nanoring structures, *Nanotechnology* 20(46), 465203 (2009)
33. C. M. Sweeney, C. L. Stender, C. L. Nehl, W. Hasan, K. L. Shuford, and T. W. Odom, Optical properties of tipless gold nanopyramids, *Small* 7(14), 2032 (2011)
34. C. S. Levin, C. Hofmann, T. A. Ali, A. T. Kelly, E. Morosan, and P. Nordlander, Magnetictplasmonic coretshell nanoparticles, *ACS Nano* 3, 1379 (2009)
35. T. Ambjornsson, G. Mukhopadhyay, S. P. Apell, and M. Kall, Resonant coupling between localized plasmons and

anisotropic molecular coatings in ellipsoidal metal nanoparticles, *Phys. Rev. B* 73, 085412 (2006)

36. W. S. Chang, J. B. Lassiter, P. Swanglap, H. Sobhani, S. Khatua, P. Nordlander, N. J. Halas, and S. A. Link, A plasmonic fano switch, *Nano Lett.* 12(9), 4977 (2012)
37. F. López-Tejeira, R. Paniagua-Domínguez, R. Rodríguez-Oliveros, and J. A. Sánchez-Gil, Fano-like interference of plasmon resonances at a single rod-shaped nanoantennas, *New J. Phys.* 14, 023035 (2012)
38. J. Zhao, J. Z. Yang, P. P. Zhu, C. Sun, and J. Xu, A comparative study of the effects of sulfate reducing bacteria on corrosion of carbon steel Q235 under simulated disbonded coating with different width of aperture, *Adv. Mater. Res.* 503–504, 247 (2012)
39. Z. Chen, R. Hu, L. Cui, L. Yu, L. Wang, and J. Xiao, Plasmonic wavelength demultiplexers based on tunable Fano resonance in coupled-resonator systems, *Opt. Commun.* 320, 6 (2014)
40. E. D. Palik, Handbook of Optical Constant of Solids, London: Academic Press, 1991
41. E. D. Palik and G. Ghosh, The Electronic Handbook of Optical Constants of Solids, London: Academic Press, 1999
42. D. M. Sullivan, Electromagnetic Simulation Using the FDTD Method, New Jersey: Wiley & Sons, 2013
43. U. S. Inan and R. A. Marshall, Numerical Electromagnetic: The FDTD Method, New York: Cambridge University Press, 2011
44. J. B. Lassiter, H. Sobhani, J. A. Fan, J. Kundu, F. Capasso, P. Nordlander, and N. J. Halas, Fano resonances in plasmonic nanoclusters: Geometrical and chemical tunability, *Nano Lett.* 10(8), 3184 (2010)
45. Y. Shao, S. Xu, X. Zheng, Y. Wang, and W. Xu, Optical fiber LSPR biosensor prepared by gold nanoparticle assembly on polyelectrolyte multilayer, *Sensors* 10(4), 3585 (2010)
46. Y.Q. Chen and C.J. Lu, Surface modification on silver nanoparticles for enhancing vapor selectivity of localized surface plasmon resonance sensors, *Sens. Actuators B* 135(2), 492 (2009)
47. J. Ye, F. Wen, H. Sobhani, J. B. Lassiter, P. V. Dorpe, P. Nordlander, and N. J. Halas, Plasmonic nanoclusters: Near field properties of the fano resonance interrogated with SERS, *Nano Lett.* 12(3), 1660 (2012)
48. E. M. Larsson, J. Alegret, M. Käll, and D. S. Sutherland, Sensing characteristics of NIR localized surface plasmon resonances in gold nanorings for application as ultrasensitive biosensors, *Nano Lett.* 7(5), 1256 (2007)
49. L. J. Sherry, S. H. Chang, G. C. Schatz, R. P. Van Duyne, B. J. Wiley, and Y. Xia, Localized surface plasmon resonance spectroscopy of single silver nanocubes, *Nano Lett.* 5(10), 2034 (2005)
50. F. Hao, Y. Sonnefraud, P. V. Drope, S. A. Maier, N. J. Halas, and P. Nordlander, Symmetry breaking in plasmonic nanocavities: Subradiant LSPR sensing and a tunable fano resonance, *Nano Lett.* 8(11), 3983 (2008)
51. N. Liu, T. Wiess, M. Mesch, L. Langguth, U. Eignthaler, M. Hirscher, C. Sönnichsen, and H. Giessen, Planar metamaterial analogue of electromagnetically induced transparency for plasmonic sensing, *Nano Lett.* 10(4), 1103 (2010)